Performance of the center-of-curvature optical assembly during cryogenic testing of the James Webb Space Telescope

James B. Hadaway[a], Conrad Wells[b], Gene A. Olczak[b], Mark Waldman[c], Tony L. Whitman[b], Joseph Cosentino[b], Michael Zarella[b], Mark Connolly[b], David M. Chaney[d], & Randal Telfer[e]

[a]University of Alabama in Huntsville, 301 Sparkman Dr., Huntsville, AL 35899
[b]Harris Corp., Space and Intelligent Systems, 400 Initiative Dr., Rochester, NY 14606
[c]Sigma Space Corp., 4600 Forbes Blvd., Lanham, MD 20706
[d]Ball Aerospace & Technologies Corp., 1600 Commerce St., Boulder, CO 80301
[e]Space Telescope Science Institute, 3700 San Martin Dr., Baltimore, MD 21218

ABSTRACT

The James Webb Space Telescope (JWST) primary mirror (PM) is 6.6 m in diameter and consists of 18 hexagonal segments, each 1.5 m point-to-point. Each segment has a 6 degree-of-freedom hexapod actuation system and a radius-of-curvature (ROC) actuation system. The full telescope was tested at its cryogenic operating temperature at Johnson Space Center (JSC) in 2017. This testing included center-of-curvature measurements of the PM wavefront error using the Center-of-Curvature Optical Assembly (COCOA), along with the Absolute Distance Meter Assembly (ADMA). The COCOA included an interferometer, a reflective null, an interferometer-null calibration system, coarse and fine alignment systems, and two displacement measuring interferometer systems. A multiple-wavelength interferometer was used to enable alignment and phasing of the PM segments. By combining measurements at two laser wavelengths, synthetic wavelengths up to 15 mm could be achieved, allowing mirror segments with millimeter-level piston errors to be phased to the nanometer level. The ADMA was used to measure and set the spacing between the PM and the focus of the COCOA null (i.e., the PM center-of-curvature) for determination of the ROC. This paper describes the COCOA, the PM test setup, the testing performed, the test results, and the performance of the COCOA in aligning & phasing the PM segments and measuring the final PM wavefront error.

Keywords: James Webb Space Telescope, JWST, primary mirror, multiple-wavelength interferometer, interferometry, cryogenic, optical testing, optical metrology.

1. INTRODUCTION

The James Webb Space Telescope, shown in Figure 1, will operate in the near to mid-infrared to observe the formation of the earliest stars and galaxies.[1] The primary mirror is 6.6 m in diameter and consists of 18 hexagonal mirror segments, each approximately 1.5 m point-to-point. The observatory will orbit the L2 point 1.5 million kilometers from Earth, away from the sun. A large sunshade will keep the telescope cold, with the primary mirror at approximately 45 K. The segments are coated with gold for high infrared reflectance. Each primary mirror segment assembly (PMSA) is constructed from a lightweight beryllium substrate with both a radius-of-curvature actuation system and a six degree-of-freedom (DOF) hexapod actuation system. The actuation systems will allow the 18 segments to be precisely aligned and adjusted in ROC once at L2 to form a phased primary mirror with the appropriate optical quality for diffraction-limited imaging at a wavelength of 2 um.

*hadawayj@uah.edu; phone 1-256-824-2533; uah.edu

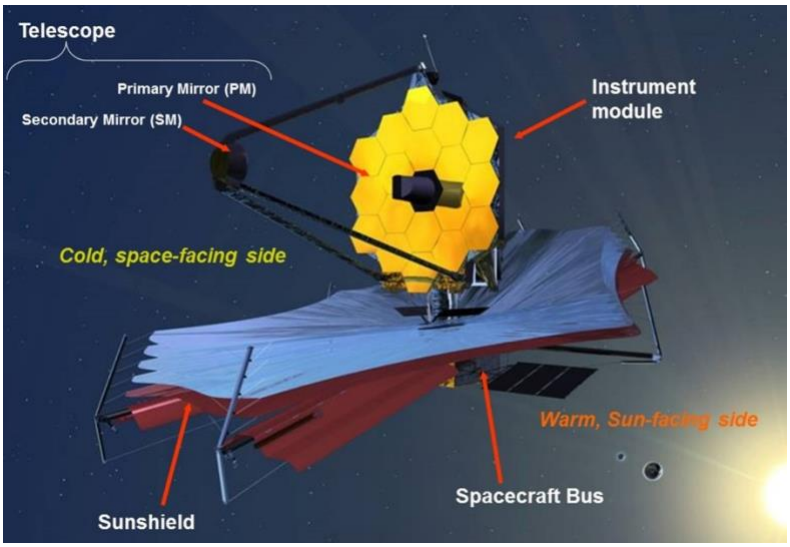

Figure 1. The James Webb Space Telescope.

The JWST Optical Telescope Element (OTE) and the Integrated Science Instrument Module (ISIM), together known as the OTIS, were tested at the cryogenic operating temperature at Johnson Space Center in 2017. The testing included center-of-curvature measurements of the PM, using the Center-of-Curvature Optical Assembly and the Absolute Distance Meter Assembly, along with the photogrammetry (PG) system. This paper describes the OTIS test setup for PM testing, the testing performed, the test results, and the metrology system performance.

2. OTIS CRYOGENIC TEST OVERVIEW

The top-level objectives of the OTIS cryogenic testing were to check the OTE & OTE-to-ISIM alignment and to assess the optical performance.[2] One of the main components of the testing was the PM center-of-curvature metrology system. This system was used to accomplish the following.

- Align the 18 PMSAs into a phased PM, with the proper ROC & conic constant.
- Align the PM globally to the Aft Optical Subsystem (AOS).
- Measure the phased PM wavefront error (WFE), ROC, and conic constant.

The measurement results were then used for the following.

- Compare the measured 1g PM WFE, ROC, and conic constant to predictions.
- Estimate the 0g PM WFE.
- Determine the PM collecting area.

In addition to the basic demonstration that the PMSAs could be aligned into a phased PM and the PM could be globally aligned to the AOS, the center-of-curvature optical metrology system was also used to check & adjust the PMSA/PM alignment, as necessary, in support of other OTIS testing, such as the pass-and-a-half testing with the science instruments.

The test configuration is illustrated on the left in Figure 2, highlighting the PM center-of-curvature test hardware (COCOA, ADMA, and PG system), along with a few other critical systems. First, the AOS Source Plate Assembly (ASPA), attached to the top of the AOS, provided upward facing fiber-fed light sources at the intermediate focus of the three-mirror telescope. The light then reflected off the secondary mirror, the PM, and then a set of three auto-collimating flats (ACFs) to provide a pass-and-a-half optical path for ISIM testing. There was also the vibration isolation system, which consisted of six down-rods attached to isolators at the top of the chamber. The OTIS, the COCOA, the ADMA, and the ACFs were all supported by the down-rods to provide vibration isolation. The optical layout of the PM center-of-curvature testing is shown on the right in Figure 2.

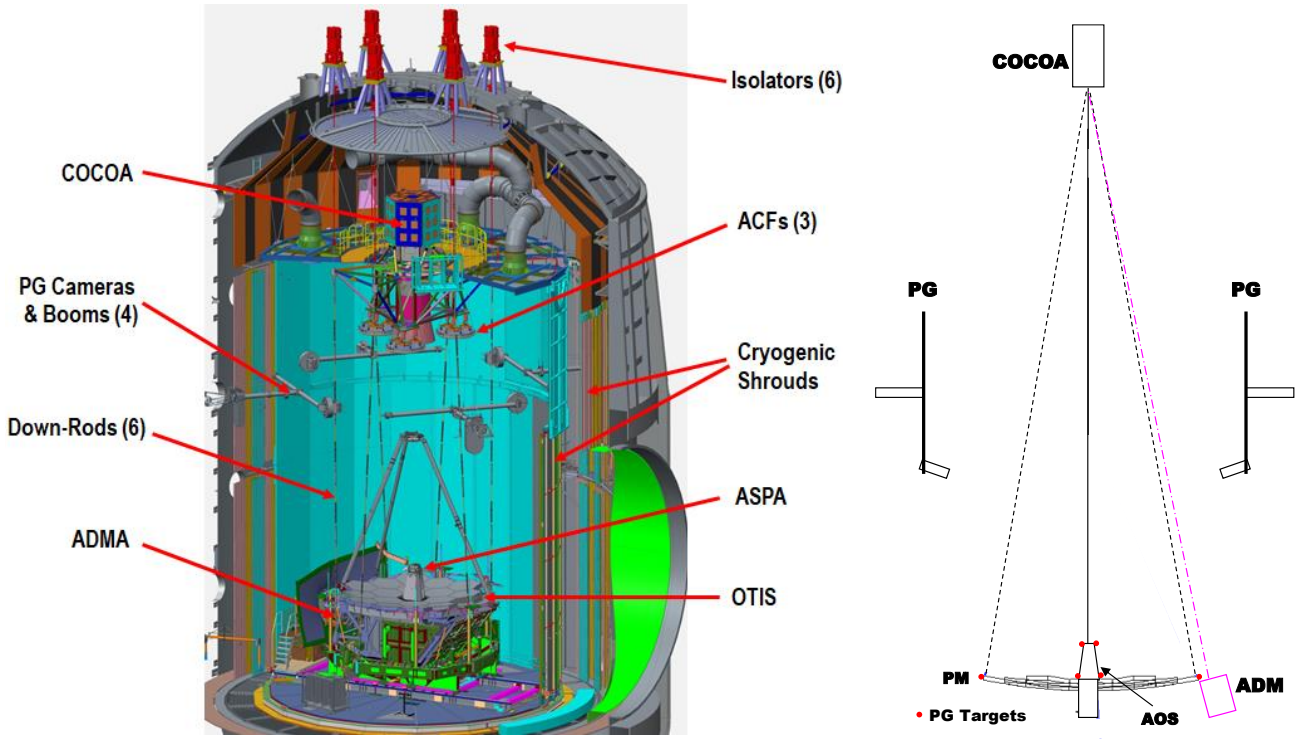

Figure 2. The OTIS test configuration and the optical layout of the PM center-of-curvature testing.

A photograph of the OTIS inside the chamber and the layout of the PM are shown in Figure 3. PG targets were installed on the exposed sides of the outer PMSAs. Displacement measuring interferometer (DMI) retro-reflectors were installed on two PMSAs, and an ADMA retro-reflector was installed on one PMSA just above the ADMA. Six Fiducial Light Array Bars (FLABs), each having two red LEDs that could be seen by the COCOA interferometer, were located around the periphery of the PM. The FLABs were used for initial pointing alignment of the COCOA to the PM.

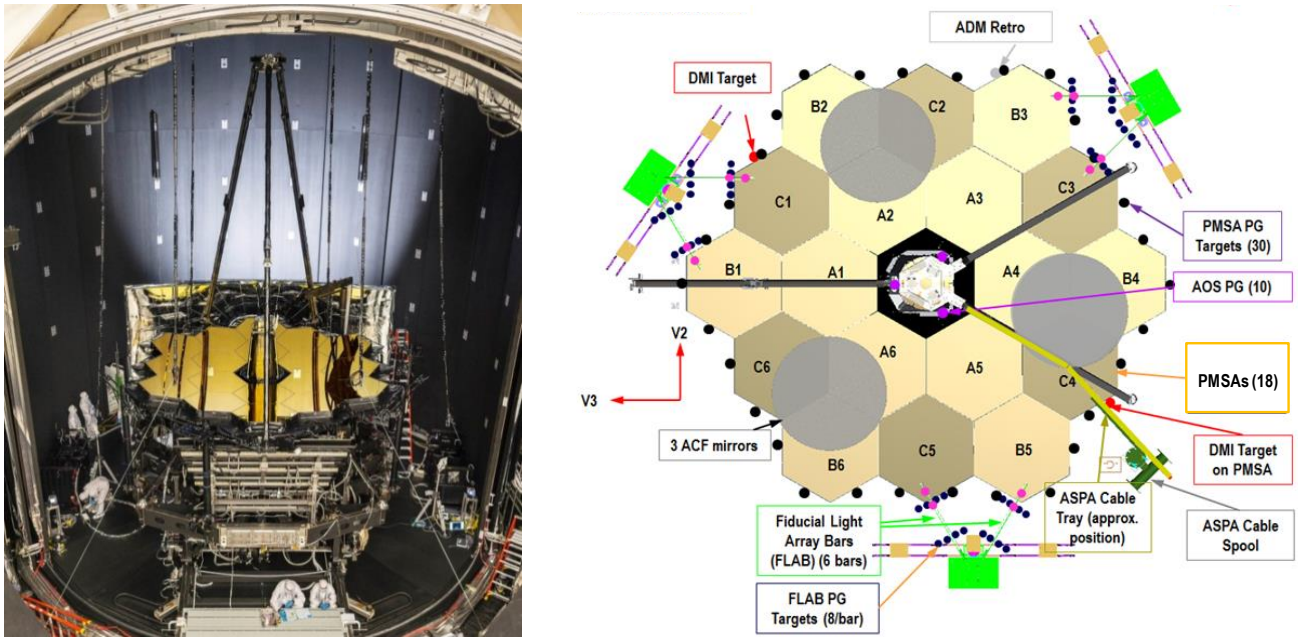

Figure 3. The OTIS in the vacuum chamber and the PM layout.

3. THE PM CENTER-OF-CURVATURE OPTICAL METROLOGY SYSTEM

As noted above, the major components of the center-of-curvature optical metrology system included the PG system, the COCOA, and the ADMA. Each will be described below.

3.1 The PG system

The PG system, as shown in Figure 4, consisted of a set of four cameras on rotating windmill booms at 90° intervals around the chamber. PG targets were attached to all of the major telescope & metrology components. The cameras collected hundreds of images as the windmills rotated. The images were then used to determine the global positions of the outer PMSAs, among other things, with respect to the AOS (the reference) to an uncertainty of <0.1 mm. The PG system was found to meet all of its measurement requirements during earlier testing.[3]

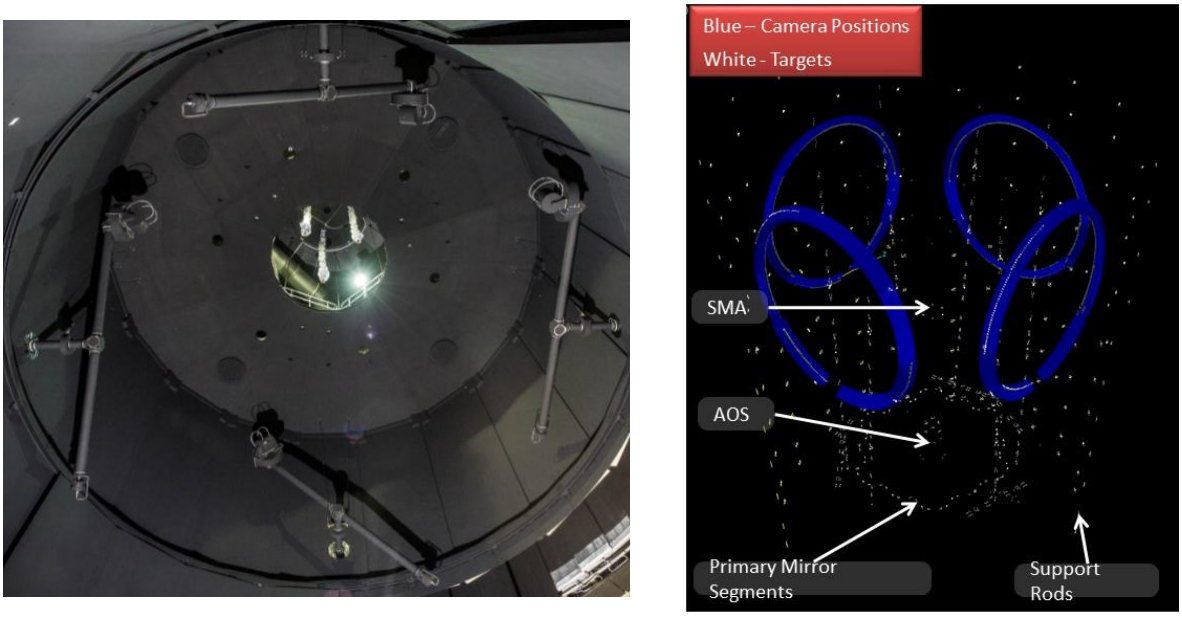

Figure 4. The PG system arrangement in the chamber and a simulation of the camera movement & PG targets.

3.2 The COCOA

The COCOA, illustrated in Figure 5, consisted of the multiple-wavelength interferometer (MWIF), a reflective null, a MWIF-null calibration subsystem, coarse & fine alignment subsystems (CASS & FASS), and a DMI subsystem.[4] The MWIF & DMIs were housed in a pressure tight enclosure (PTE) since they were not vacuum compatible. A hexapod motion subsystem provided the capability to position the COCOA in six degrees-of-freedom. And a thermal control subsystem, consisting of multi-layer insulation, heater panels, and a thermal shutter, was used to maintain the internal COCOA temperature at 291 K while in the cryogenic environment. The COCOA was located in an LN_2 environment above the gaseous helium shroud.

The MWIF was an instantaneous phase-shifting interferometer with multi-wavelength capability, designed for segmented mirror measurements. It had two single-wavelength lasers (687 nm & 660 nm) and one tunable wavelength laser (680-690 nm). Measurements could be made at the fundamental laser wavelength of 687 nm and at synthetic wavelengths from 16.8 um to 15 mm, produced by combining two measurements made at separate laser wavelengths. This range of wavelengths allowed phasing of the PMSAs in piston from several mm down to the nm level. The use of polarized light and a polarizing mask bonded to the interferometer CCD enabled phase-shifted data to be captured during a single camera exposure for each wavelength, with only 10 usec between the two exposures. This minimized the impact of vibration between the COCOA and the PM on the measured WFE.

A computer-generated hologram (CGH) could be periodically inserted at the paraxial focus of the null to measure, or calibrate, the MWIF/null WFE for removal from the PM WFE measurements.

Lastly, the DMIs were used to monitor the COCOA-to-PM axial spacing during certain phases of the test.

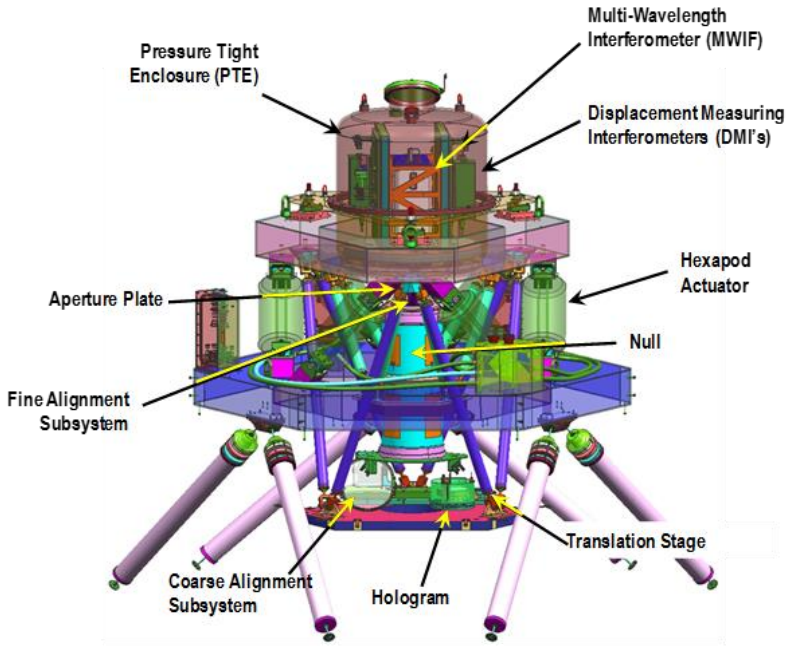

Figure 5. The COCOA (thermal shutter and external heater panels & shrouds not shown).

Software developed by Harris, the Segmented Aperture Software Suite (SASS), was used to process the raw images from the MWIF camera. This software generated the PM WFE maps and the COCOA and PMSA adjustments (rigid-body & ROC) required for the alignment & phasing. The COCOA was aligned in translation to minimize global PM tilt and in rotation, about the PM center-of-curvature, to minimize global PM coma, while maintaining a constant COCOA-to-PM axial distance. The PMSAs were aligned in position & ROC to minimize the WFE, with the COCOA adjustments accounted for in the calculations.

3.3 The ADMA

As indicated in Figure 2 above, the ADMA was positioned just beneath the PM, and faced upward. A drawing of the ADMA is given on the right in Figure 6. It was used, along with the PG system, to set the PM-to-COCOA axial distance. This was done by measuring the distance to a corner cube mounted to the edge of one of the outer PMSAs and to a cube mounted inside the COCOA, with a known offset from the COCOA paraxial focus. Photogrammetry supported the process by measuring the global locations of the ADMA & the PM. Risley prisms inside the ADMA were used to steer the measurement beam to each corner cube. The geometry of the measurements is shown on the left in Figure 6.

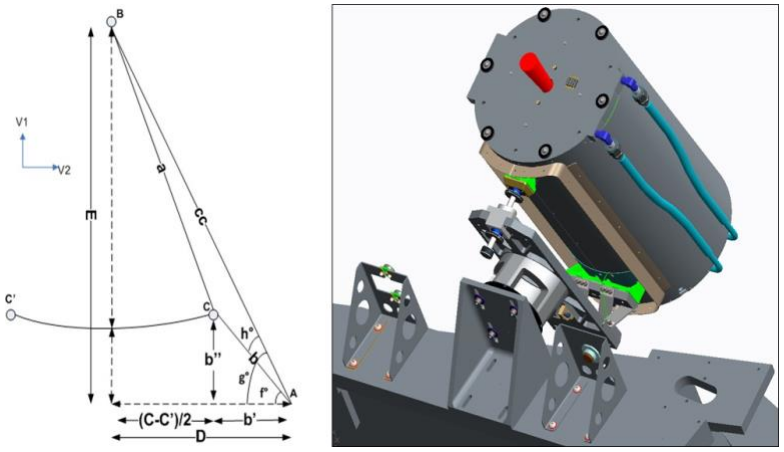

Figure 6. The PM-to-COCOA axial distance geometry and the ADMA.

4. PM ALIGNMENT

In the subsections below, an outline of the PM alignment process will first be presented, followed by the results of the "run-for-the-money" PM alignment, consisting of the PMSA alignment & phasing and the PM global alignment, performed during the OTIS cryogenic test.

4.1 The PM alignment process

The top-level process for aligning & measuring the PM was as follows.

- Use the PG system to globally align the outer 12 PMSAs (only ones with PG targets) to the AOS.
- Use the COCOA CASS, FASS, and FLABs to initially align the COCOA to the PM (outer 12 PMSAs) and to initially align the PMSAs in tilt.
- Use the ADMA to set the COCOA-to-PM axial distance to the nominal paraxial ROC.
- Use the COCOA MWIF to fine align the COCOA to the PM and to fully align & phase the PMSAs in all degrees-of-freedom, with periodic checks/adjustments of the axial distance via the ADMA.
- Use the PG system to check the PM global alignment. If out of tolerance, then correct global position and repeat the COCOA & PMSA alignment steps above.
- When all alignment tolerances are met, make the final PM WFE measurement with the MWIF and the final axial distance/ROC measurement with the ADMA.

This alignment process, along with all of the associated hardware, control software, and data processing software, was checked and refined during a series of three optical ground-support equipment (OGSE) tests performed in 2015 & 2016.[5] The testing was performed using the Pathfinder OTE, consisting of a non-flight primary mirror backplane center section & secondary mirror support structure, two spare PMSAs, the spare secondary mirror assembly, and either the AOS simulator (first & third tests) or the flight AOS (second test). This testing was invaluable in preparing for the flight OTIS test.

4.2 PMSA alignment results

The "run-for-the-money" PM alignment was performed before any other testing just after stable cryogenic conditions were achieved. The results of this alignment are presented below. The PM was subsequently realigned as necessary for other testing.

Following the initial global alignment of the outer 12 PMSAs using the PG system, as will be detailed in the next section, the PMSA alignment & phasing was performed.

Since a PM alignment had been performed during the latter part of the chamber cool-down, there was no need to use the CASS or the FLABs for this alignment.

The COCOA & PMSA alignment using the FASS was performed without any issues.

Next, the COCOA-to-PM axial distance was set to the nominal value of 15,879.222 mm using the ADMA with an error of -52 um, well within the tolerance of ±125 um.

The alignment process then continued using the MWIF. The initial stage consisted of the following steps.

- COCOA aligned only in decenter, using only outer PMSAs, due to large PMSA tilts.
- PMSAs aligned only in tilt to reduce fringe density.
- Alignment iterated until <10 tilt fringes (<2.3 urad total tilt) on each PMSA.

The next stage consisted of the following steps.

- COCOA aligned in all DOFs, using only outer PMSAs.
- PMSAs aligned initially only in piston & tilt.

- Synthetic wavelengths included in MWIF measurements stepped down from longer to shorter as PMSA piston reduced.
- After initial larger PMSA piston & tilt and COCOA corrections completed, ROC added to PMSA DOFs of piston & tilt.
- After initial larger PMSA ROC corrections completed, and COCOA alignment very close to tolerances, radial decenter & clocking added to PMSA DOFs (i.e., all but tangential decenter).
- Alignment iterated until COCOA alignment tolerances met and all PMSA misalignments well below global position tolerances (i.e., 100 um), with PMSA piston within capture range of 0.5 mm synthetic wavelength and PMSA tilts < ±1 urad (5 fringes).

The final stage consisted of the following steps.

- COCOA aligned in all DOFs, using all PMSAs, since inner PMSAs now well aligned to outer PMSAs.
- PMSAs aligned only in piston, tilt, and ROC.
- Synthetic wavelengths included in MWIF measurements stepped down from longer to shorter as PMSA piston reduced, ending with 16.8 um wavelength.
- Alignment iterated until all COCOA & PMSA alignment tolerances met.

The final PMSA alignment was 118 nm-PV (34 nm-rms) in piston, ≤83 nrad in tilt, and ≤10 nm-PV in power/ROC. The alignment convergence in terms of total PM WFE was excellent, as shown in Figure 7. Not all of the iterations are shown in the figure since some were used to move only a subset of the PMSAs, some were used only for COCOA moves, etc. The increase after iteration 3 was due to the large PMSA decenter & clocking moves made at that time, which led to large residual piston & tilt errors, which were then corrected in the following iterations.

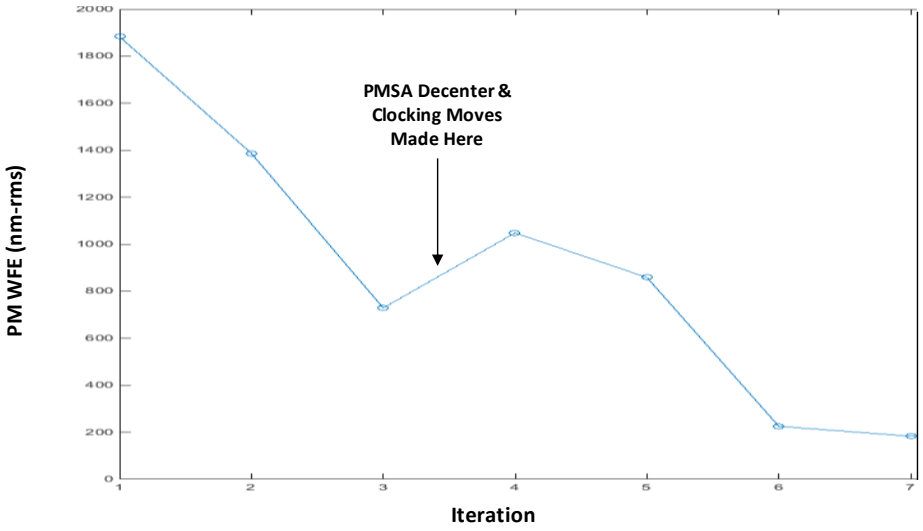

Figure 7. PM WFE convergence during the alignment.

4.3 PM global alignment results

As the first step in the overall PM alignment process, the outer 12 PMSAs, the ones with PG targets, were successfully aligned to the AOS using the PG system. All of the alignment tolerances were met, as shown in Table 1.

Table 1. Initial PM global alignment.

DOF	Starting	Ending	Tolerance
Piston (mm)	-0.325	-0.014	±0.084
Decenter (mm)	0.163	0.031	±0.030
Clocking (mrad)	-0.023	-0.013	±0.697
Tilt (mrad)	0.182	0.006	±0.079

The PM global alignment from PG measurements made after the alignment using the MWIF is shown in Table 2. It showed that the PM had been inadvertently misaligned globally in decenter by 0.451 mm during the alignment using the MWIF. While this was well outside the decenter tolerance, it was decided that the global misalignment would not prevent any of the future testing, especially the pass-and-a-half testing, from being successfully completed, and that sufficient data had been gathered to assess the PMSA poses for flight. Also, the ability to properly align the PM to the AOS had already been demonstrated, both during the cool-down and during the initial setting during this alignment. Thus, correction of the misalignment was deemed to be unnecessary.

Table 2. Final PM global alignment.

DOF	Measured	Tolerance
Piston (mm)	-0.016	±0.084
Decenter (mm)	0.451	±0.030
Clocking (mrad)	-0.036	±0.697
Tilt (mrad)	0.065	±0.079

The cause of the misalignment was determined, during the test, to be the manner in which the COCOA DOFs were set in the SASS code during data processing. In addition to the six rigid-body DOFs, there was an ROC DOF for the COCOA. Since the axial distance was set using the ADMA and the SASS used the piston DOF to keep the axial distance fixed for any lateral translations or tilts of the COCOA, it was believed that the ROC DOF did not need to be included in the calculations. This belief was reinforced by good results for COCOA alignment seen during the Pathfinder testing, when the ROC DOF was not used. But, there were only two PMSAs on the Pathfinder. It turned out that for the case of a full 18 PMSA mirror, the lack of the ROC DOF caused the singular value decomposition matrices for the alignment calculations to be ill-conditioned. As a result, the COCOA pointing calculations were incorrect. And since the COCOA rotated about the PM paraxial center-of-curvature, global PM coma was not properly removed by the COCOA alignment. The only remaining means available to correct the coma was for the PM to move as whole in decenter to align itself to the incorrectly pointed COCOA.

5. PM MEASUREMENT RESULTS

The results of the measurements of the fully aligned PM, including the 1g WFE, ROC, conic constant, and collecting area, are presented in the subsections below, along with a comparison of the measured 1g WFE to that predicted and an estimation of the 0g WFE.

5.1 1g WFE

A fringe image and the final PM WFE are shown in Figure 8. Note that the WFE is dominated by the gravity deformation of the extremely light-weighted PMSAs. This deformation is dominated by power, which is removed using the ROC actuator, leaving a trefoil-dominated shape due to the three support whiffles on the back of the PMSA. Also note that some of the PMSAs were partially obscured by the secondary mirror support struts, the secondary mirror mount, an ASPA fiber cable tray arm, and the FLABs. The only obscuration in flight will be the struts, with the others due to GSE and the COCOA's view from the PM center-of-curvature.

Excellent alignment was achieved, with a final PM WFE of 183 nm-rms, close to the 158 nm-rms predicted by the optimized optical model.

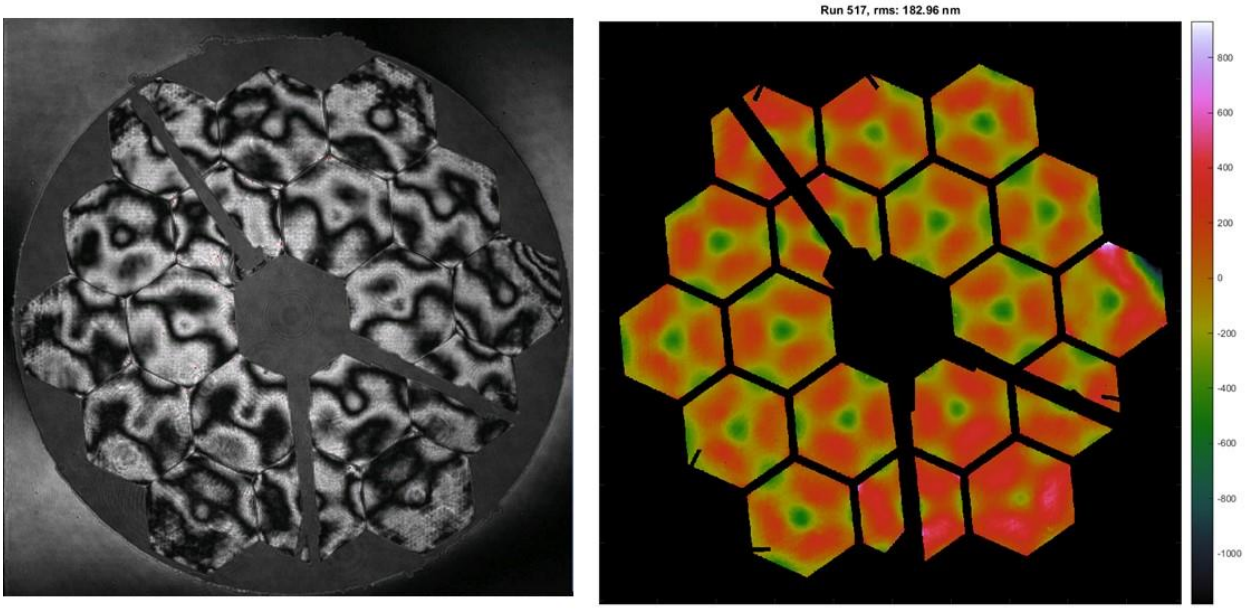

Figure 8. Fringe image & WFE map for the fully aligned PM.

Of note, however, is the WFE on the PMSA at the far right in the figures above, which was unusual in shape and was higher than expected. This was eventually determined to be from entanglement of a PG target attached to the upper-right edge of the PMSA with the PMSA closeout structure, which led to deformation of the mirror surface. However, this will not be an issue for flight since the PG targets will not be present.

5.2 ROC, conic constant, and collecting area

The COCOA-to-PM axial distance determined using the ADMA & PG data after the alignment was used, along with the residual PM Zernike power & spherical aberration, to calculate the PM ROC and conic constant. The results, along with the estimated worst-case 2-sigma uncertainties, are shown in Table 3. The delta from nominal was very low for both, and the uncertainties met the requirements.

Table 3. Final measured PM ROC & conic constant.

Parameter	Measured Value	Delta from Nominal	Estimated Uncertainty	Required Uncertainty
ROC (mm)	15,879.209	-0.013	±0.350	±0.400
Conic Constant	-0.996692	-32 ppm	±21 ppm	±200 ppm

See reference 6 for further details on the ROC & conic measurement process and data processing.

The results of two measurements were used to determine the PM collecting area, as seen from the center-of-curvature. The first was a fringe modulation map from the final PM WFE measurement, as shown in Figure 9. This was used to determine the number of valid WFE pixels on the MWIF camera. The second measurement used was an image of the COCOA LEDs on the FLABs that was recorded on the MWIF camera following the final PM WFE measurements. This, along with PG data, was used to determine the scale of the MWIF pixels at the PM.

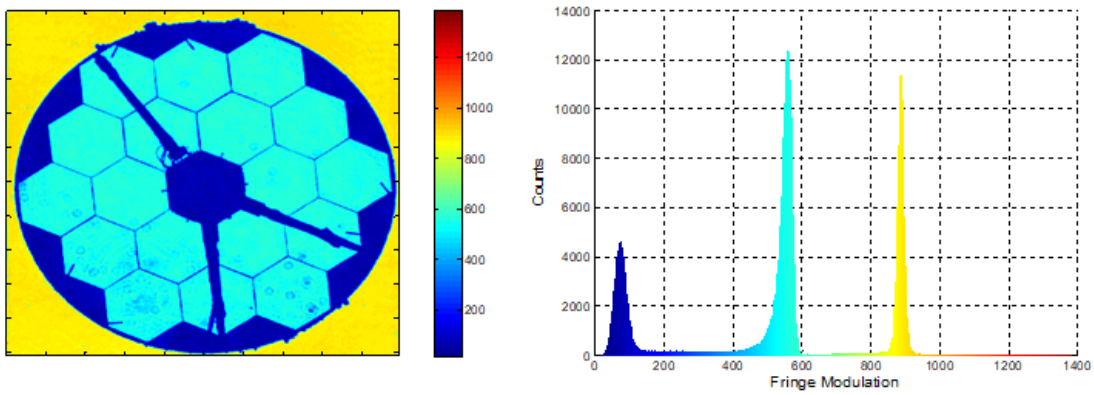

Figure 9. PM fringe modulation data used in determining the PM collecting area.

For the COCOA perspective, the predicted PM collecting area was 25.054 m^2, with an uncertainty of +4.3%/-4.2%. The pixel scale determined using the FLAB image was 7.09406 mm/px. The PM collecting area determined from the final MWIF measurement was 25.411 m^2, which matches the predicted area to 1.4%. This was well within the uncertainty of the prediction and below the measurement uncertainty requirement of ≤5%.

5.3 Measured versus predicted 1g WFE

As a cross-check of the PM WFE, the measured 1g WFE was compared to that predicted. The prediction was generated by combining the 0g WFE measured previously during PMSA final acceptance testing (PMSA mounted horizontally) with the vertical gravity deformation predicted via a structural model. The difference between the measured & predicted WFE's is shown in Figure 10. The PMSA deformed by the PG target entanglement, as described in Section 5.1, was excluded. Residual PMSA alignment aberrations (tilt, power, & astigmatism) have been removed from the measured WFE, and the fit of the maps has been optimized for lateral alignment & scale, on a PMSA-by-PMSA basis. The resulting difference of 25.8 nm-rms was within the estimated combined prediction/measurement/registration uncertainty of 26 nm-rms.

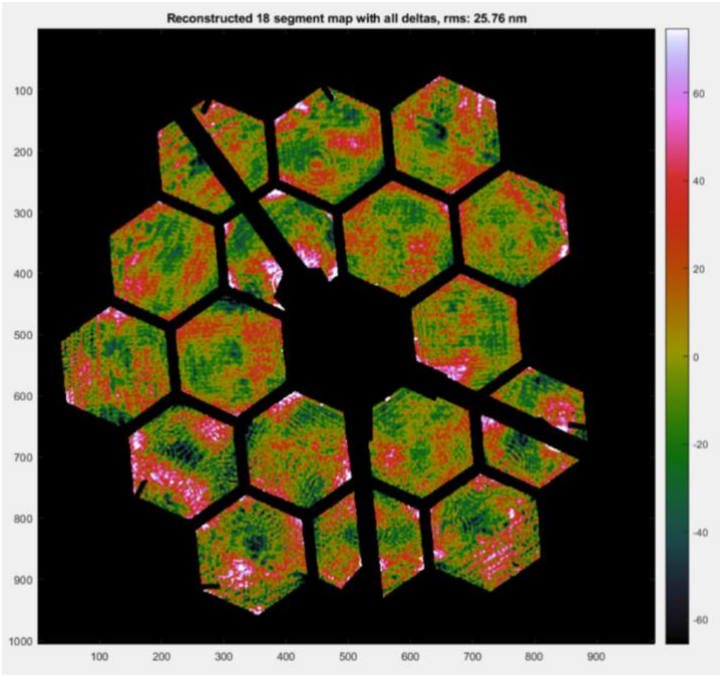

Figure 10. The difference between the measured & predicted PM 1g WFE.

5.4 Estimated 0g WFE

An estimate of the 0g PM WFE was generated by analytically removing the 1g deformation of each PMSA from the measured 1g WFE. As in the comparison of the 1g WFE to that predicted, the residual PMSA alignment aberrations have been removed from the measured WFE, and the fit of the maps has been optimized for lateral alignment & scale, on a PMSA-by-PMSA basis. The resulting 0g PM WFE map estimated from the 1g measurement made during this testing is shown on the left in Figure 11, with the predicted 0g PM WFE map shown on the right. There is excellent visual and magnitude correlation, with 37 nm-rms WFE estimated compared to 39 nm-rms predicted.

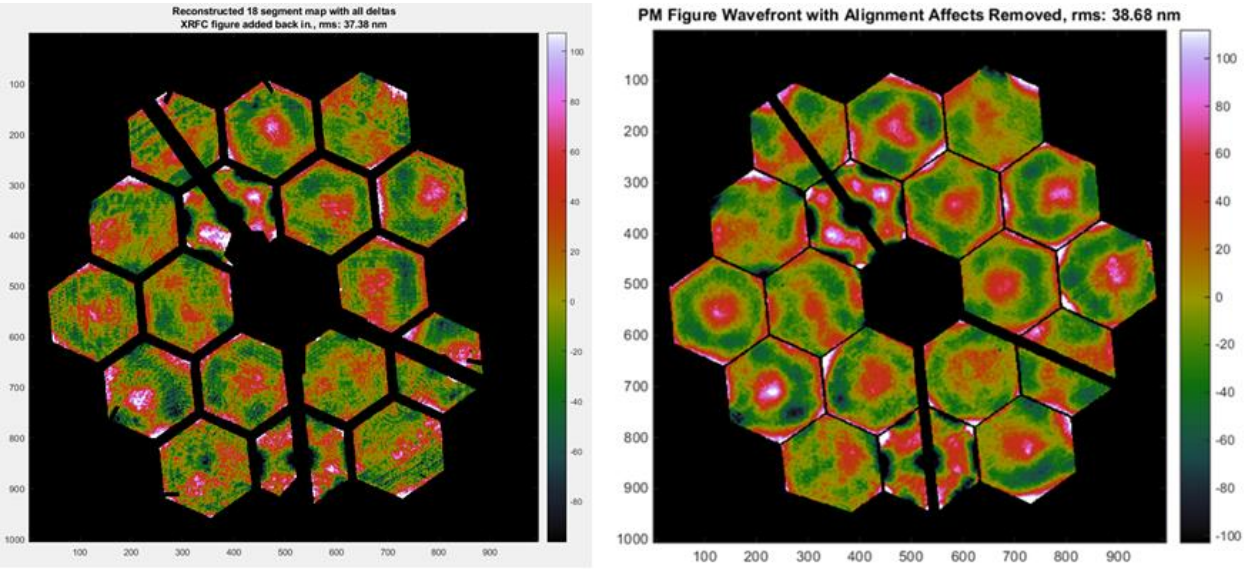

Figure 11. The PM 0g WFE estimated from the 1g measurement (left) and the predicted 0g WFE (right).

6. SUMMARY & CONCLUSIONS

All of the test objectives for the PM testing using the center-of-curvature optical metrology system were accomplished.

- Aligned the 18 PMSAs into a phased PM, with the proper ROC & conic constant.
- Aligned the PM globally to the AOS.
- Measured the phased PM WFE, ROC, and conic constant.
- Aligned PM sufficiently for all other testing.

All of the test requirements were met

- The measured 1g PM WFE matched the prediction to within the combined uncertainty.
- The measured PM ROC & conic constant were within the required uncertainties of their nominal values.
- The estimated 0g PM WFE was in excellent agreement with the prediction.
- The PM collecting area calculated from the measured WFE matched the prediction to within the required uncertainty.

ACKNOWLEDGEMENTS

The design, preparation, and execution of this test were supported by the JWST contract NNG11FD64C with NASA Goddard Space Flight Center (GSFC). The JWST system is a collaborative effort involving NASA, ESA, CSA, the astronomy community and numerous principal investigators. The cryogenic test and analysis were accomplished through

the efforts of NASA GSFC, NASA JSC, Northrop Grumman Aerospace Systems, Harris Space and Intelligence Systems, Ball Aerospace and Technologies, and the Space Telescope Science Institute.

REFERENCES

[1] Lightsey, P. A., Atkinson, C., Clampin, M., and Feinberg, L. D., "James Webb Space Telescope: large deployable cryogenic telescope in space," Opt. Eng. 51 (1), 011003 (2012).

[2] Feinberg, L. D., Barto, A., Waldman, M., and Whitman, T. L., "James Webb Space Telescope system cryogenic optical test plans," Proc. SPIE 8150, (2011).

[3] Lunt, S., Rhodes, D., DiAntonio, A., Boland, J., Wells, C., Gigliotti, T., and Johanning, G., "Model predictions and observed performance of JWST's cryogenic position metrology system," Proc. SPIE 9904, 99044C (2016).

[4] Wells, C., Olczak, G., Merle, C., Dey, T., Waldman, M., Whitman, T., Wick, E., and Peer, A., "The center of curvature optical assembly for the JWST primary mirror cryogenic optical test," Proc. SPIE 7739, 77390L (2010).

[5] Hadaway, J. B., Wells, C., Olczak, G., Waldman, M., Whitman, T., Cosentino, J., Connolly, M., Chaney, D., and Telfer, R., "Performance of the primary mirror center-of-curvature optical metrology system during cryogenic testing of the JWST Pathfinder telescope," Proc. SPIE 9904, 99044E (2016).

[6] Cosentino, J., Wells, C., Olczak, G., and Hadaway, J. B., "Setting the James Webb Space telescope primary mirror radius of curvature and conic constant during cryogenic testing", Proc. SPIE 10698, (2018).